Synthesis, Characterization, and Magnetic Properties of Two New Co(II) Coordination Polymers with a Carboxylate- and Benzimidazolyl-containing Ligand

Xiao-Chun Cheng and Hai-Wei Kuai

Faculty of Life Science and Chemical Engineering, Huaiyin Institute of Technology, Huaian 223003, P. R. China

Reprint requests to Dr. Hai-Wei Kuai. Fax: +86-517-83559044. E-mail: hyitshy@126.com

Z. Naturforsch. **2012**, *67b*, 1255 – 1262 / DOI: 10.5560/ZNB.2012-0235
Received August 22, 2012

The hydrothermal reaction of cobalt(II) nitrate hexahydrate with 5-(benzimidazol-1-ylmethyl)isophthalic acid (H_2L) leads to the formation of a complex [Co(L)] (**1**). In the presence of 2-(pyridin-2-yl)-1*H*-benzimidazole (pybim) as an auxiliary ligand, a complex [Co(L)(pybim)]·H_2O (**2**) was obtained. The complexes **1** and **2** have been characterized by single-crystal and powder X-ray diffraction, IR spectroscopy, and elemental and thermogravimetric analyses. Complex **1** shows a binodal (3,6)-connected 2D **kgd** network with $(4^3)_2(4^6.6^6.8^3)$ topology; **2** shows a chain structure, further linked together by hydrogen bonding and π–π interactions to give rise to a 3D supramolecular framework. Complexes **1** and **2** are examples of auxiliary ligand-assisted structural diversity. The frameworks of **1** and **2** display high thermal stability up to 400 °C. The magnetic properties of **1** were investigated.

Key words: Co(II) Complexes, Structural Characterization, Auxiliary Ligand, Magnetic Properties

Introduction

During the past decades, synthesis and characterization of metal-organic frameworks (MOFs), involving metal ions and bridging ligands, have attracted increasing interest and undergone considerable development in coordination, materials and supramolecular chemistry [1 – 5]. Consequently, a large number of MOFs were prepared [6 – 9], and the exploitation of such inorganic-organic hybrid materials has gradually become the main aim of crystal engineering for their intriguing topologies and potential applications in magnetism, heterogeneous catalysis, ion-recognition, nonlinear optics, and adsorption [10 – 12]. It is known that the functional properties of complexes are closely related with their structures, and thus, it becomes significant to pursue structural diversity by attempting different experimental conditions though it is still a great challenge to assemble complexes with target structures because of complicated factors influencing the assembly process, such as solvent, reaction temperature, and auxiliary ligands *etc*. [13 – 15]. However, the complexity of self-assembly may also give access to composite polymers with novel functional properties as a vast domain of potentially multifunctional materials [16 – 18]. Among many influential factors, the intrinsic nature of organic ligands has been proven to play a decisive role in the formation of complexes [19 – 21].

With this background in mind, we have recently focused our attention on the utilization of the carboxylate- and benzimidazol-1-yl-containing ligand 5-(benzimidazol-1-ylmethyl)isophthalic acid (H_2L) as a building block for the construction of coordination polymers with diverse structures. H_2L can be readily synthesized, and its molecular structure has previously been determined by single-crystal X-ray diffraction [22, 23]. Due to the existence of two functional groups, the arene-cored ligand H_2L exhibits advantages over other *N*- or *O*-donor ligands for its peculiar structural characteristics: (1) because of the relative orientation of two carboxylate groups and their mutable coordination patterns such as μ_1-η^1:η^0-monodentate, μ_1-η^1:η^1-chelating and μ_2-η^1:η^1-bridging modes [24, 25], H_2L can act as a multi-connector in the assembly of complexes with various structures; (2) the flexible benzimidazol-

1-ylmethyl arm in H_2L has more spatial freedom to adopt different orientations by axial rotation to different angles to satisfy coordinating requirements [26–28], and furthermore, (3), the steric hindrance of the benzimidazol-1-yl group may engender a subtle impact on the formation of complexes. For this contribution, two cobalt complexes [Co(L)] (**1**) and [Co(L)(pybim)]·H_2O (**2**) (pybim = 2-(pyridin-2-yl)-1*H*-benzimidazole) were synthesized under hydrothermal conditions and characterized by single-crystal and powder X-ray diffraction, IR spectroscopy, and elemental and thermogravimetric analyses. In addition, the magnetic properties of **1** were also investigated.

Results and Discussion

Preparation

The hydrothermal reaction of $Co(NO_3)_2·6H_2O$ with H_2L at 180 °C in the presence of KOH yielded the complex [Co(L)] (**1**); when pybim was introduced into the hydrothermal reaction system as auxiliary ligand, the complex [Co(L)(pybim)]·H_2O (**2**) was obtained (Scheme 1). Complexes **1** and **2** are stable in air.

*Structural description of [Co(L)] (**1**)*

Structural analysis shows that complex **1** crystallizes in the monoclinic system with space group $P2_1/c$ exhibiting a 2D network structure (Table 1). The H_2L ligand was deprotonated by KOH to the L^{2-} anion. This can also be confirmed in the IR spectrum by the absence of a characteristic vibration band for -OH near 3400 cm^{-1} for anhydrous **1**, and the presence of characteristic vibration bands of carboxylates at 1621 cm^{-1} for asymmetric stretches and at 1453 cm^{-1} for symmetric stretches (see Experimental Section). The asymmetrical unit contains one Co(II) ion and one L^{2-} ligand. Each Co(II) center is four-coordinated by

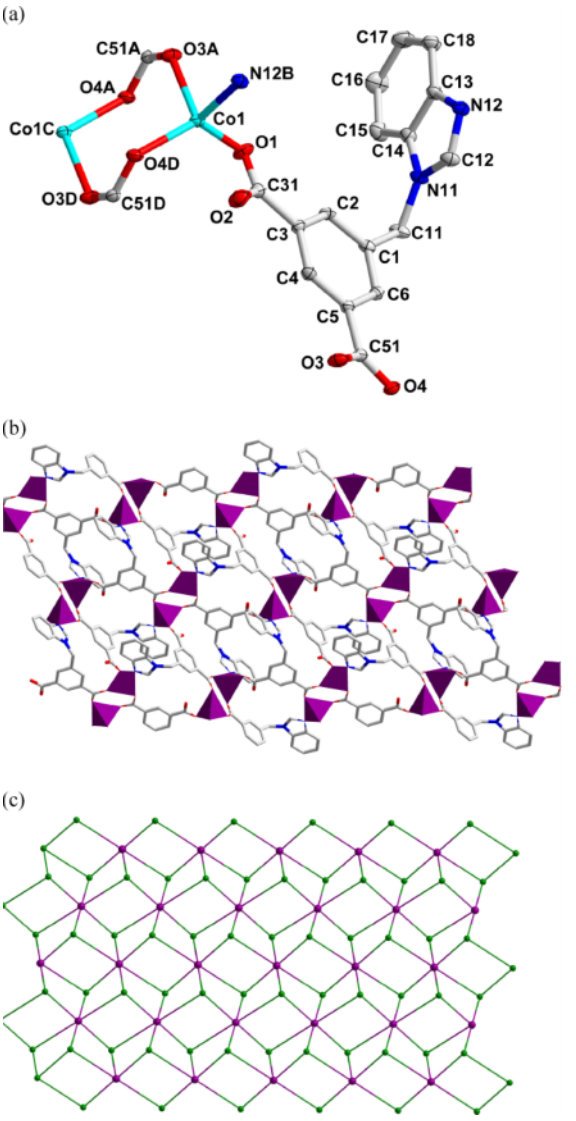

Fig. 1. (a) The coordination environment of the Co atom in **1** with 30 % displacement ellipsoids. Hydrogen atoms were omitted for clarity; (b) view of 2D network structure of **1**; (c) schematic representation of the binodal (3,6)-connected 2D network of **1**.

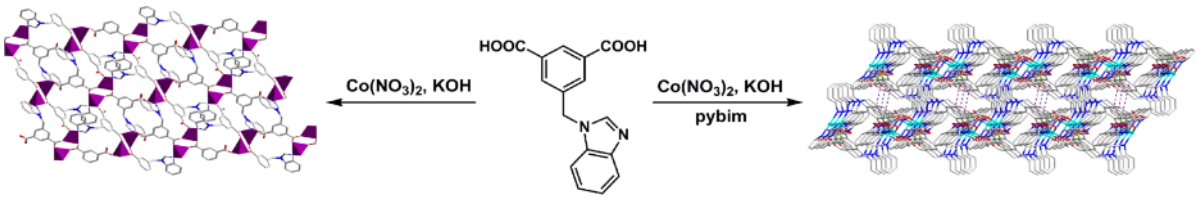

Scheme 1. Simplified representation of the synthesis and structures of **1** and **2**.

Table 1. Crystal structure data for **1** and **2**.

	1	**2**
Formula	$C_{16}H_{10}CoN_2O_4$	$C_{28}H_{21}CoN_5O_5$
M_r	353.19	566.43
Crystal size, mm^3	$0.20 \times 0.20 \times 0.20$	$0.20 \times 0.10 \times 0.10$
Crystal system	monoclinic	triclinic
Space group	$P2_1/c$	$P\bar{1}$
a, Å	8.3072(10)	9.9364(7)
b, Å	11.3306(13)	10.2290(7)
c, Å	16.9473(16)	13.7624(9)
α, deg	90.0	77.8000(10)
β, deg	119.352(4)	81.6940(10)
γ, deg	90.0	64.0920(10)
V, Å^3	1390.4(3)	1227.64(14)
Z	4	2
D_{calcd}, g cm^{-3}	1.69	1.53
μ(Mo K_α), cm^{-1}	1.3	0.8
F(000), e	716	582
hkl range	±10, ±14, $-22 \rightarrow +9$	$-12 \rightarrow 13$, $-13 \rightarrow +11$, ±18
θ range, deg	2.27 – 28.00	1.52 – 28.39
Refl. measured / unique / R_{int}	8508 / 3290 / 0.0311	8863 / 6052 / 0.0127
Param. refined	208	350
$R(F)$[a] / $wR(F^2)$[b] (all refls.)	0.0391 / 0.0871	0.0459 / 0.1104
GoF (F^2)[c]	1.059	1.060
$\Delta\rho_{fin}$ (max / min), e Å^{-3}	0.37 / −0.42	0.91 / −0.42

[a] $R(F) = \Sigma||F_o| - |F_c||/\Sigma|F_o|$; [b] $wR(F^2) = [\Sigma w(F_o^2 - F_c^2)^2/\Sigma w(F_o^2)^2]^{1/2}$, $w = [\sigma^2(F_o^2) + (AP)^2 + BP]^{-1}$, where $P = (\mathrm{Max}(F_o^2,0) + 2F_c^2)/3$; [c] GoF $= [\Sigma w(F_o^2 - F_c^2)^2/(n_{obs} - n_{param})]^{1/2}$.

Table 2. Selected bond lengths (Å) and angles (deg) for complexes **1** and **2**[a].

[Co(L)] (**1**)			
Co(1)–O(1)	2.0386(15)	Co(1)–O(4)#1	2.0056(14)
Co(1)–N(12)#2	2.0307(17)	Co(1)–O(3)#3	1.9989(14)
O(1)–Co(1)–O(4)#1	125.61(6)	O(1)–Co(1)–N(12)#2	112.00(7)
O(1)–Co(1)–O(3)#3	101.19(6)	O(4)#1–Co(1)–N(12)#2	111.60(7)
O(3)#3–Co(1)–O(4)#1	106.55(6)	O(3)#3–Co(1)–N(12)#2	94.00(6)
[Co(L)(pybim)]·H_2O (**2**)			
Co(1)–N(3)	2.1579(17)	Co(1)–N(4)	2.0954(15)
Co(1)–N(11)	2.1119(16)	Co(1)–O(3)#1	2.0266(15)
Co(1)–O(1)#2	2.2778(17)	Co(1)–O(2)#2	2.1561(15)
N(3)–Co(1)–N(4)	77.49(6)	N(3)–Co(1)–N(11)	169.14(6)
O(3)#1–Co(1)–N(3)	87.41(7)	O(1)#2–Co(1)–N(3)	94.05(7)
O(2)#2–Co(1)–N(3)	93.10(7)	N(4)–Co(1)–N(11)	93.26(6)
O(3)#1–Co(1)–N(4)	117.29(7)	O(1)#2–Co(1)–N(4)	96.43(6)
O(2)#2–Co(1)–N(4)	153.04(7)	O(3)#1–Co(1)–N(11)	91.92(7)
O(1)#2–Co(1)–N(11)	92.62(6)	O(2)#2–Co(1)–N(11)	97.69(6)
O(1)#2–Co(1)–O(3)#1	145.63(6)	O(2)#2–Co(1)–O(3)#1	86.99(6)
O(1)#2–Co(1)–O(2)#2	58.64(6)		

[a] Symmetry transformations used to generate equivalent atoms: for **1**: #1 $1-x$, $1/2+y$, $3/2-z$; #2 $-x$, $1-y$, $1-z$; #3 $-1+x$, $3/2-y$, $-1/2+z$; for **2**: #1 $1+x$, $-1+y$, z; #2 $1-x$, $1-y$, $1-z$.

one benzimidazolyl nitrogen atom and three carboxylate oxygen atoms from three different L^{2-} ligands to furnish a distorted tetrahedral coordination geometry [$CoNO_3$] (Fig. 1a). The coordinative bond lengths vary from 1.9989(14) to 2.0386(15) Å, and the coordinating bond angles are in the range from 94.00(6) to 125.61(6)° (Table 2). One of the carboxylate groups in the L^{2-} ligand adopts μ_1-η^1:η^0−monodentate coordination mode, the other is in a μ_2-η^1:η^1-bridging coordination mode [Scheme 2(A)], resulting in the forma-

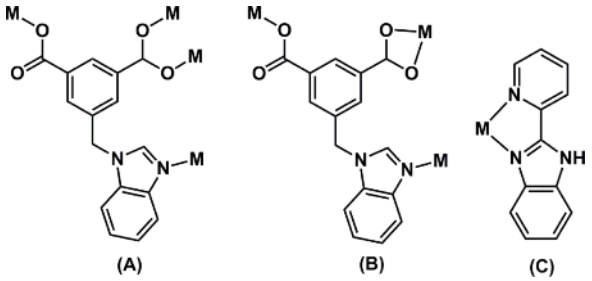

Scheme 2. The coordination modes of the L^{2-} and the pybim ligands appearing in the complexes.

tion of carboxylate-bridged binuclear secondary building unit (SBU) [$Co_2(COO)_2$] with a Co···Co distance of 3.80 Å (Fig. 1a), which is shorter than the sum of two van der Waals radii (3.84 Å). This indicates that there may be Co···Co contacts within the binuclear units. In complex **1**, each L^{2-} ligand bridges three SBUs; each SBU is surrounded by six L^{2-} ligands. This kind of connection repeats infinitely to form 2D network structure (Fig. 1b). Topology can be used to further analyze the structure of **1**, each SBU being regarded as a 6-connector node and each L^{2-} ligand as a 3-connector node. Thus, the resultant structure of **1** could be simplified as a binodal (3,6)-connected 2D **kgd** network with $(4^3)_2(4^6.6^6.8^3)$ topology (Fig. 1c) [29].

*Structural description of [Co(L)(pybim)]·H_2O (**2**)*

The complex [Co(L)(pybim)]·H_2O (**2**) crystallizes in the triclinic crystal system with space group $P\bar{1}$ and is composed of neutral chains and water molecules. The asymmetric unit consists of one Co(II) cation,

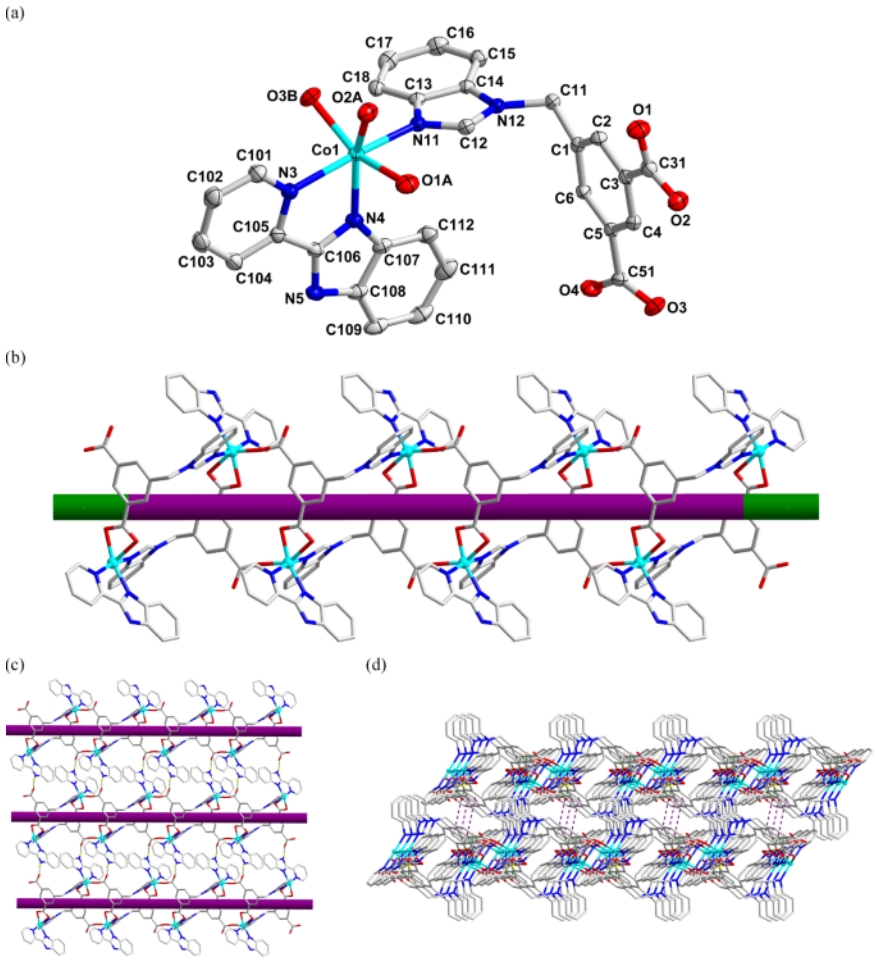

Fig. 2. (a) The coordination environment of the Co atom in **2** with 30% displacement ellipsoids. Hydrogen atoms and the water molecule were omitted for clarity; (b) view of the 1D structure of **2**; (c) the 2D network of **2** extended by hydrogen bonds; (d) the extended 3D supramolecular framework of **2**.

one L^{2-} anion, one pybim molecule, and one disordered water molecule. The coordination environment around the Co atom is shown in Fig. 2a together with the atom numbering scheme. The Co atom is hexacoordinated with distorted octahedral coordination geometry by three carboxylate O atoms from two different L^{2-} ligands, one benzimidazolyl N atom, and two N atoms from a pybim molecule [Scheme 2(B) and (C)]. The equatorial plane is occupied by three carboxylate O atoms with an average Co–O bond length of 2.154 Å and one pybim N atom; the two axial positions are held by benzimidazolyl and pybim N atoms with Co–N bond lengths of 2.1119(16) and 2.1579(17) Å; the coordinative bond angles at Co vary from 58.64(6) to 169.14(6)°. In complex **2**, one carboxylate group of the L^{2-} ligand exhibits a μ_1-η^1:η^0-monodentate coordination mode, while the other is μ_1-η^1:η^1-chelating with the angle subtended at cobalt being 58.64(6)°; each benzimidazolyl group coordinates to a metal center, and thus the whole L^{2-} ligand adopts a μ_3-η^1:η^0-η^1:η^1-η^1 mode as a 3-connector bridge; each metal center is coordinated by three different L^{2-} ligands. The interconnection of metal and ligand extends infinitely to form a neutral chain structure (Fig. 2b). Apart from the coordinative bonds, hydrogen bonding and π–π stacking interactions are present in **2**, which undoubtedly play an important role in constructing and stabilizing the resulting solid-state structure. According to their function in constructing a supramolecular structure, we divide the weak interactions into two groups: (1) N(5)–H(19)···O(4)#1 [#1: $1-x, 1-y, 2-z$; N(5)···O(4)#1 = 2.746(2) Å; ∠N(5)–H(19)···O(4)#1 = 164°], the hydrogen bonding interactions between H atoms in pybim molecules and carboxylate O atoms from adjacent chains, which further link these chains to form a 2D network (Fig. 2c); (2) π–π stacking interactions with a centroid-centroid distance between the central benzene rings of 3.979 Å, through which adjacent 2D networks are superposed to yield a 3D supramolecular framework (Fig. 2d).

*PXRD and thermal stability of complexes **1** and **2***

The phase purities of **1** and **2** could be proven by powder X-ray diffraction (PXRD). As shown in Fig. 3, each PXRD pattern of the as-synthesized sample is consistent with the simulated one.

Thermogravimetric analyses (TGA) were carried out for complexes **1** and **2**, and the results of TGA are shown in Fig. 4. No obvious weight loss can be observed before the decomposition of the framework at 530 °C for **1**, which further confirms that no solvent is trapped in its structure. For complex **2**, there is a weight loss of 2.90 % from 85 °C to 150 °C corresponding to the release of water (calcd. 3.18 %), preceding the subsequent decomposition of the framework at 400 °C.

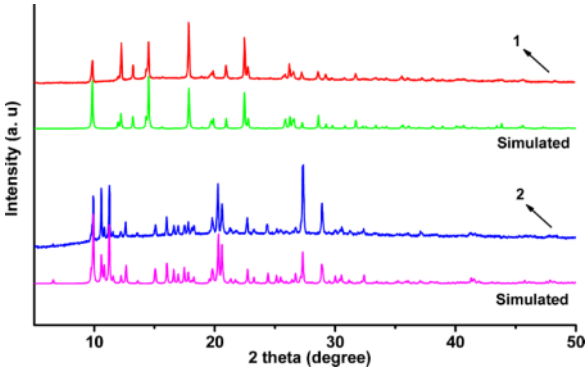

Fig. 3. The PXRD patterns of complexes **1** and **2**.

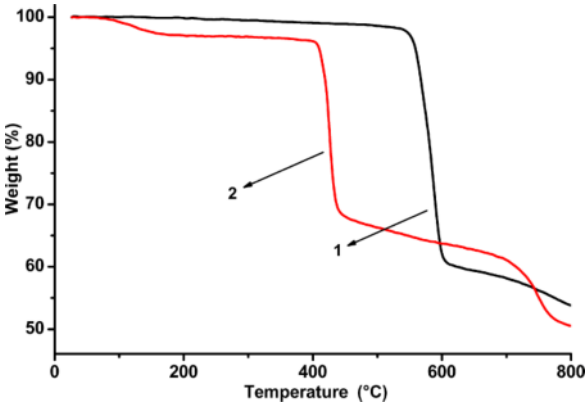

Fig. 4. TGA curves of complexes **1** and **2**.

*Magnetic properties of complex **1***

The Co atoms are bridged by carboxylate groups to form a dinuclear unit $[Co_2(COO)_2]$ in **1**, which may mediate magnetic interactions [30]. The temperature dependence of the magnetic susceptibility of **1** was investigated from 300 to 1.8 K with an applied magnetic field of 2000 Oe. The χ_M, χ_M^{-1}, and $\chi_M T$ *vs.* T curves for **1** are shown in Fig. 5. The temperature dependence of χ_M^{-1} above 50 K obeys the Curie-Weiss equation of $\chi_M^{-1} = (T - \theta)/C$ with the Curie-Weiss constants $C = 3.36$ cm^3 mol^{-1} K, $\theta = -40.45$ K.

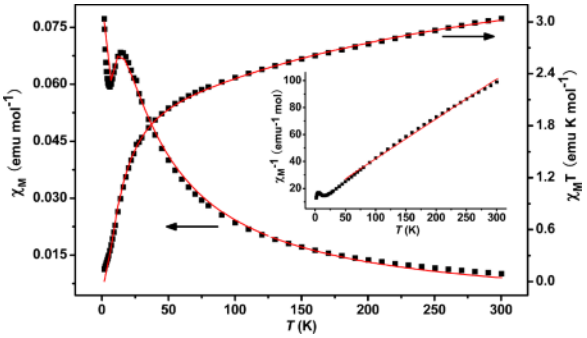

Fig. 5. Temperature dependences of the magnetic susceptibility of χ_M, χ_M^{-1} and $\chi_M T$ for **1**. The solid line represents the fitted curve.

The negative value of θ and the shape of the $\chi_M T$ *vs.* T curve suggest antiferromagnetic interactions between the neighboring Co(II) centers [31 – 33]. In order to estimate the strength of the magnetic interactions in **1**, the following equation was used [34, 35]:

$$\chi_M T = Ae^{(-E1/kT)} + Be^{(-E2/kT)} \quad (1)$$

Here, $A+B$ approximately equals the Curie constant (C), and E_1, E_2 represent the 'activation energies' corresponding to the spin-orbit coupling and the magnetic exchange interaction, respectively. The obtained values of $A+B=3.39$ cm^3 mol^{-1} K and $E_1/k=48.96$ K agree with those given in a previous report [34, 35]. The value of $-E_2/k=-1.39$ K, corresponding to $J=-2.78$ K, further proves that antiferromagnetic interaction exists between neighboring Co atoms in **1** [36, 37].

Conclusion

The ligand 5-(benzimidazol-1-ylmethyl)isophthalic acid (H_2L) reacts with cobalt nitrate hexahydrate under hydrothermal conditions to yield the complex [Co(L)] (**1**). In the presence of the auxiliary ligand pybim, the complex [Co(L)(pybim)]·H_2O (**2**) is formed. Complex **1** is a binodal (3,6)-connected 2D **kgd** network with $(4^3)_2(4^6.6^6.8^3)$ topology; **2** shows a chain structure, further linked by hydrogen bonding and π–π interactions to form a 3D supramolecular framework. Structural diversity is thus achieved by the presence of an auxiliary ligand. The frameworks of **1** and **2** exhibit high thermal stability up to 400 °C. Investigation of magnetic properties shows antiferromagnetic interactions between neighboring Co atoms in **1**.

Experimental Section

All commercially available chemicals were reagent grade and used as received without further purification. The H_2L ligand was synthesized *via* a similar experimental procedure as reported in the literature (Scheme 3) [22]. Elemental analysis of C, H, and N were taken on a Perkin-Elmer 240C elemental analyzer. Infrared spectra (IR) were recorded on a Bruker Vector22 FT-IR spectrophotometer by using KBr pellets. Thermogravimetric analysis (TGA) was performed on a simultaneous SDT 2960 thermal analyzer under nitrogen atmosphere with a heating rate of 10 °C min^{-1}. Powder X-ray diffraction (PXRD) patterns were measured on a Shimadzu XRD-6000 X-ray diffractometer with Cu K_α ($\lambda=1.5418$ Å) radiation at room temperature. The magnetic measurement in the temperature range of 1.8 to 300 K was carried out on a Quantum Design MPMS7 SQUID magnetometer in a field of 2 kOe (1 kOe $=7.96\times10^4$ A m^{-1}).

*Preparation of [Co(L)] (**1**)*

The reaction mixture of $Co(NO_3)_2{\cdot}6H_2O$ (29.1 mg, 0.1 mmol), H_2L (29.6 mg, 0.1 mmol) and KOH (11.2 mg, 0.2 mmol) in 12 mL H_2O was sealed in a 16 mL Teflon-lined stainless-steel container and heated at 180 °C for 48 h. After cooling to r. t., red block-shaped crystals of **1** were collected by filtration and washed with water and ethanol several times to give a yield of 52 % based on H_2L. – $C_{16}H_{10}N_2O_4Co$ (353.19): calcd. C 54.41, H 2.85, N 7.93; found C 54.66, H 2.98, N 8.16. – IR (KBr pellet, cm^{-1}): $\nu=1621$ (s), 1565 (s), 1509 (s), 1453 (s), 1377 (s), 1241 (w), 1185 (w), 1104 (w), 967 (w), 917 (w), 806 (w), 775 (w), 760 (s), 740 (s), 725 (s), 674 (w), 649 (w), 593 (w), 532 (w).

*Preparation of [Co(L)(pybim)]·H_2O (**2**)*

Complex **2** was obtained by an analogous hydrothermal procedure as that used for the preparation of **1** except that pybim (19.5 mg, 0.1 mmol) was used as an auxiliary ligand. After cooling to room temperature, red block-shaped crystals of **2** were collected by filtration and washed with water and ethanol several times to give a yield of 56 % based on H_2L. – $C_{28}H_{21}N_5O_5Co$ (566.43): calcd. C 59.37, H 3.74, N 12.36;

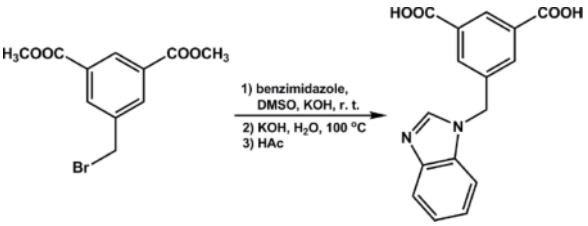

Scheme 3. Schematic representation of the synthetic route of the H_2L ligand.

found C 59.62, H 3.96, N 12.13. – IR (KBr pellet, cm^{-1}): $\nu = 3437$ (m), 1611 (s), 1571 (s), 1544 (s), 1504 (m), 1477 (m), 1459 (s), 1441 (s), 1384 (s), 1321 (m), 1299 (m), 1183 (w), 978 (m), 750 (s), 715 (s).

X-Ray structure determinations

The crystallographic data collections for complexes **1** and **2** were carried out on a Bruker Smart Apex CCD area-detector diffractometer using graphite-monochromatized MoK_α radiation ($\lambda = 0.71073$ Å) at 293(2) K. The diffraction data were integrated by using the program SAINT [38], which was also used for the intensity corrections for Lorentz and polarization effects. Semi-empirical absorption corrections were applied using SADABS [39]. The structures of **1** and **2** were solved by Direct Methods, and all non-hydrogen atoms were refined anisotropically on F^2 by full-matrix least-squares techniques using the SHELXS/L-97 crystallographic software package [40, 41]. In **1** and **2**, all hydrogen atoms at C atoms were generated geometrically; the hydrogen atoms of the water molecule in **2** could not be located and thus were excluded from the refinement, while the H19 at N5 in **2** could be found at a reasonable position in the difference Fourier maps. The details of crystal parameters, data collection, and refinements for the complexes are summarized in Table 1. Selected bond lengths and angles are listed in Table 2.

CCDC 896724 and 896725 contain the supplementary crystallographic data for this paper. These data can be obtained free of charge from The Cambridge Crystallographic Data Centre *via* www.ccdc.cam.ac.uk/data_request/cif.

[1] G. C. Xu, Q. Hua, T. Okamura, Z. S. Bai, Y. J. Ding, Y. Q. Huang, G. X. Liu, W. Y. Sun, N. Ueyama, *Cryst EngComm* **2010**, *11*, 261 – 270.

[2] T. Uemura, Y. Ono, Y. Hijikata, S. Kitagawa, *J. Am. Chem. Soc.* **2010**, *132*, 4917 – 4924.

[3] C. Y. Chen, J. Peng, Y. Shen, D. Chen, H. Q. Zhang, C. L. Meng, *Z. Naturforsch.* **2011**, *66b*, 43 – 48.

[4] G. C. Liu, J. X. Zhang, X. L. Wang, H. Y. Lin, A. X. Tian, Y. F. Wang, *Z. Naturforsch.* **2011**, *66b*, 125 – 132.

[5] L. F. Ma, X. Q. Li, L. Y. Wang, H. W. Hou, *CrystEngComm* **2011**, *13*, 4625 – 4634.

[6] Y. Kobayashi, B. Jacobs, M. D. Allendorf, J. R. Long, *Chem. Mater.* **2010**, *22*, 4120 – 4122.

[7] M. S. Chen, Z. Su, M. Chen, S. S. Chen, Y. Z. Li, W. Y. Sun, *CrystEngComm* **2010**, *2*, 3267 – 3276.

[8] J. F. Kou, M. Su, Y. H. Zhang, Z. D. Huang, S. W. Ng, G. Yang, *Z. Naturforsch.* **2010**, *65b*, 1467 – 1471.

[9] C. Kallfaß, C. Hoch, H. Schier, A. Simon, H. Schubert, *Z. Naturforsch.* **2010**, *65b*, 1427 – 1433.

[10] J. R. Li, R. J. Kuppler, H. C. Zhou, *Chem. Soc. Rev.* **2009**, *38*, 1477 – 1504.

[11] B. L. Chen, S. C. Xiang, G. D. Qian, *Acc. Chem. Res.* **2010**, *43*, 1115 – 1124.

[12] B. H. Ye, M. L. Tong, X. M. Chen, *Coord. Chem. Rev.* **2005**, *249*, 545 – 565.

[13] S. Mishra, E. Jeanneau, H. Chermette, S. Daniele, L. G. Hubert-Pfalzgraf, *Dalton Trans.* **2008**, 620 – 630.

[14] Z. He, C. He, E. Q. Gao, Z. M. Wang, X. F. Yang, C. S. Liao, C. H. Yan, *Inorg. Chem.* **2003**, *42*, 2206 – 2208.

[15] B. Zhao, L. Yi, Y. Dai, X. Y. Chen, P. Cheng, D. Z. Liao, S. P. Yan, Z. H. Jiang, *Inorg. Chem.* **2005**, *44*, 911 – 920.

[16] L. F. Ma, L. Y. Wang, D. H. Lu, S. R. Batten, J. G. Wang, *Cryst. Growth Des.* **2009**, *9*, 1741 – 1749.

[17] Z. Su, J. Fan, T. Okamura, W. Y. Sun, N. Ueyama, *Cryst. Growth Des.* **2010**, *10*, 3515 – 3521.

[18] W. W. Zhou, J. T. Chen, G. Xu, M. S. Wang, J. P. Zou, X. F. Long, G. J. Wang, G. C. Guo, J. S. Huang, *Chem. Commun.* **2008**, 2762 – 2764.

[19] G. Z. Liu, S. H. Li, L. Y. Wang, *CrystEngComm* **2012**, *14*, 880 – 889.

[20] G. X. Liu, Y. Q. Huang, Q. Chu, T. A. Okamura, W. Y. Sun, H. Liang, N. Ueyama, *Cryst. Growth Des.* **2008**, *8*, 3233 – 3245.

[21] R. Cao, D. Sun, Y. Liang, M. Hong, K. Tatsumi, Q. Shi, *Inorg. Chem.* **2002**, *41*, 2087 – 2094.

[22] J. Fan, B. E. Hanson, *Inorg. Chem.* **2005**, *44*, 6998 – 7008.

[23] X. C. Cheng, *Acta Crystallogr.* **2011**, *E67*, o3299.

[24] Z. F. Tian, J. G. Lin, Y. Su, L. L. Wen, Y. M. Liu, H. Z. Zhu, Q. J. Meng, *Cryst. Growth Des.* **2007**, *7*, 1863 – 1867.

[25] Q. Hua, Y. Zhao, G. C. Xu, M. S. Chen, Z. Su, K. Cai, W. Y. Sun, *Cryst. Growth Des.* **2010**, *10*, 2553 – 2562.

[26] H. W. Kuai, X. C. Cheng, X. H. Zhu, *J. Coord. Chem.* **2011**, *64*, 1636 – 1644.

[27] H. W. Kuai, X. C. Cheng, X. H. Zhu, *J. Coord. Chem.* **2011**, *64*, 3323 – 3332.

[28] H. W. Kuai, X. C. Cheng, L. D. Feng, X. H. Zhu, *Z. Anorg. Allg. Chem.* **2011**, *637*, 1560 – 1565.

[29] V. A. Blatov, A Multipurpose Crystallochemical Analysis with the Program Package TOPOS, Samara State University, Samara (Russia) **2009**; See also: V. A. Blatov, *IUCr CompComm Newsletter* **2006**, *7*, 4 – 38.

[30] D. Ghoshal, G. Mostafa, T. K. Maji, E. Zangrando, T. H. Lu, J. Ribas, N. R. Chaudhuri, *New J. Chem.* **2004**, *28*, 1204 – 1213.

[31] J. W. Raebiger, J. L. Manson, R. D. Sommer, U. Geiser, A. L. Rheingold, J. S. Miller, *Inorg. Chem.* **2001**, *40*, 2578 – 2581.

[32] J. M. Herrera, A. Bleuzen, Y. Dromzée, M. Julve, F. Lloret, M. Verdaguer, *Inorg. Chem.* **2003**, *42*, 7052 – 7059.
[33] Z. Su, Z. S. Bai, J. Xu, T. Okamura, G. X. Liu, Q. Chu, X. F. Wang, W. Y. Sun, N. Ueyamab, *CrystEngComm* **2009**, *11*, 873 – 880.
[34] J. M. Rueff, N. Masciocchi, P. Rabu, A. Sironi, A. Skoulios, *Chem. Eur. J.* **2002**, *8*, 1813 – 1820.
[35] J. M. Rueff, N. Masciocchi, P. Rabu, A. Sironi, A. Skoulios, *Eur. J. Inorg. Chem.* **2001**, 2843 – 2848.
[36] R. L. Carlin, *Magnetochemistry*, Springer, Berlin, Heidelberg, **1986**.
[37] O. Kahn, *Molecular Magnetism*, VCH, Weinheim, **1993**.
[38] SAINT, Program for Data Extraction and Reduction, Bruker Analytical X-ray Instruments Inc., Madison, Wisconsin (USA) **2001**.
[39] G. M. Sheldrick, SADABS, Program for Empirical Absorption Correction of Area Detector Data, University of Göttingen, Göttingen (Germany) **1997**.
[40] G. M. Sheldrick, SHELXS/L-97, Programs for Crystal Structure Determination, University of Göttingen, Göttingen (Germany) **1997**.
[41] G. M. Sheldrick, *Acta Crystallogr.* **2008**, *A64*, 112 – 122.